**ChemistryOpen**

Full Papers
doi.org/10.1002/open.202100070

**Chemistry Europe**
European Chemical
Societies Publishing

# Distinguishable Targeting of Non-Small Cell Lung Cancer Using Hyaluronan Functionalized Platinum Nanoclusters and Their Inhibition Behaviors of Proliferation, Invasion, Migration

Ting Liu[+],[a] Xin Huang[+],[b] Lingyun Zhao,[a] Zhongqing Xiao,[a] Zengbei Li,[b] Yi Xin,[c] Shanshan Yang,[a] Di Guo,[a] Wenfei Zhao,[a] Yang Mi,[d] and Hongyun Li*[a]

Lung cancer is the leading cause of cancer deaths worldwide and most cancer patients receiving conventional chemotherapy suffer from severe side effects due to the non-selective effects of chemotherapeutic drugs on normal cells. Targeted nano-materials can obtain excellent accumulation at the tumor site through their active or passive targeting mechanisms, thereby reducing the toxicity of the drugs in various ways. In this study, hyaluronic acid (HA) which could specifically bind to CD44 on the surface of tumor cells, was used to modify amine-caged platinum nanoclusters (Pt NCs-NH$_2$) to obtain targeting HA-Pt NCs-NH$_2$. Based on the differential expression of CD44 on the surface of three lung cells (non-small cell lung cancer cell H1299, small cell lung cancer cell H446, and embryonic lung fibroblast HFL1), HA-Pt NCs-NH$_2$ can differentially enter the three cells and achieve their targeting of non-small cell lung cancer cell (NSCLC) cells. Pt NCs significantly inhibited the proliferation, migration and invasion of NSCLC cells and induced their apoptosis in comparison of classical cisplatin and carboplatin, showing a bright future in early diagnosis and treatment of NSCLC.

## 1. Introduction

The latest global oncology statistics in 2018 showed that the highest cancer incidence worldwide is lung cancer, accounting for 11.6% of the total population.[1] Among the effective treatment of lung cancer, chemotherapy remains a dominating means, especially for non-small cell lung cancer (NSCLC).[2]

[a] T. Liu,[+] L. Zhao, Z. Xiao, S. Yang, D. Guo, W. Zhao, Prof. H. Li
Department of Respiratory and Critical Care Medicine
The Fifth Affiliation Hospital of Zhengzhou University
No. 3 Kangfuqian Street
Zhengzhou 450052 (China)
E-mail: lhyhxk@163.com

[b] Prof. X. Huang,[+] Z. Li
School of Textiles
Zhongyuan University of Technology
No. 41 Zhongyuan Road (M)
Zhengzhou 450007 (China)

[c] Y. Xin
Intensive Care Unit
Zhengzhou Orthopedics Hospital
No. 56 Longhai Road
Zhengzhou 450052 (China)

[d] Dr. Y. Mi
Henan Key Laboratory for Helicobacter pylori & Microbiota and GI Cancer
Marshall Medical Research Centre
The Fifth Affiliated Hospital of Zhengzhou University
No. 3 Kangfuqian Street
Zhengzhou 450052 (China)

[+] These authors contributed equally to this work.

Supporting information for this article is available on the WWW under https://doi.org/10.1002/open.202100070

However, most patients receiving conventional chemotherapy suffer from severe side effects due to the non-selective effects of chemotherapy medications on normal cells. Over the past decades, nanomaterials like nanoparticles (NPs) and nano-clusters (NCs) have been developed as drug delivery systems for various chemotherapeutic agents to enhance drug efficacy and safety.[3] Drug targeted therapy can overcome the difficulties in therapeutic delivery, especially for the accurate anchoring onto the location of tumor. In vitro and vivo studies revealed that targeted nanomaterials can achieve superior accumulation at the tumor site through their active or passive targeting mechanism to improve the selectivity during the cellular uptake process, and decline the cytotoxicity in comparison with conventional chemotherapeutic drugs and non-targeted nanoparticle platforms.[4]

Depend on the high therapeutic efficacy and less side effects,[5] it is of great importance to develop functionalized nanomaterials which could specifically bind with cell surface receptors or molecules to engage and interfere with cell signaling pathways, thereby inducing cellular regulation and removing diseased cells.[6] Targeted ligands include hyaluronic acid (HA), protein/peptide, folic acid, antibody fragment, carbohydrate/polysaccharide, etc.[7] Among them, HA is a polymeric straight-chain glycan composed of N-acetyl-D glucosamine and D-glucuronide,[8] and its major binding receptor is a single genetically encoded transmembrane protein named CD44 (cluster of differentiation 44).[9] The interaction between HA molecules and CD44 can trigger multiple intracellular signaling pathways leading to adhesion, migration, invasion and growth of tumor cells.[10] CD44 is often detected on the surface of tumor stem cells and essential for the development of malignant transformation of tumors. Meanwhile, CD44 may

ChemistryOpen

Full Papers
doi.org/10.1002/open.202100070

Chemistry
Europe
European Chemical
Societies Publishing

be a potential diagnostic target for cancer prognosis, helping to achieve early diagnosis and treatment of cancer.[11] HA-drug bioconjugates, such as HA-Taxol, HA-CPT11, HA-paclitaxel (PTX) and HA-polymer conjugates could exert potent antiproliferative activity against cancer cells which are CD44 overexpressed, including human breast, colon, ovarian, gastric, breast, oesophageal and lung cancer.[12] More importantly, nanomaterials can also be modified with HA in order to target the CD44 receptors. Mice inoculated with hepatocellular carcinoma cells were orally administered different doses of HA-selenium nanoparticles which showed the lower toxicity and significantly reduced tumor weight compared to the 5-fluorouracil-positive group.[13] Besides, HA-coated superparamagnetic iron oxide nanoparticles (HA-SPIONs) enhanced the efficacy of the anticancer drug Adriamycin (DOX). The HA-Adriamycin nanoparticles were more widely distributed in tumor tissue than intravenous free Adriamycin, leading to tumor growth inhibition and prolonging the life span of these mice.[14] Yoon et al. have successfully synthesized targeted HA nanoparticles (Ce6-HANPs) for simultaneous tumor photodynamic imaging and therapy.[15] Similarly, HA-encapsulated siRNA nanoparticles and epigallocatechin-3-gallate have been used in the studies of anti-ovarian and anti-prostate cancer, respectively.[12,16] However, the target recognition and inhibition mechanism of HA-modified nanomaterials for lung cancer have been rarely reported.

In our previous study, we found that Pt NCs can be used as fluorescent markers for selective fluorescence imaging of hematological K562 and BV173 cancer cells in contrast to peripheral blood mononuclear cells (PBMC, normal cells of the hematological system). Moreover, Pt NCs could inhibit the proliferation of hematopoietic malignancy cells by the pro-apoptotic proteins p53, PUMA and cleaved caspases, showing great potential for the diagnosis and treatment of hematological disorders.[17] Li groups found that Pt NCs-based drugs could easily access A549 and A549/DDP cells, thus enabling biological imaging of NSCLC cells as fluorescent markers. Compared to cisplatin, Pt NCs-based chemotherapeutic agents significantly inhibited the proliferation of NSCLC cells and showed superior inhibitory and apoptotic effects on cisplatin-resistant A549/DDP cells.[18] Therefore, Pt NCs apply an inspiring probability to achieve targeted identification and therapy for NSCLC *via* forming HA-functioned Pt NCs bioconjugates.

Herein, we propose to use HA to modify the amine-caged Pt NCs (Pt NCs-NH$_2$) to form multi-functional HA-Pt NCs-NH$_2$. NSCLC cells H1299, small cell lung cancer (SCLC) cells H446 and normal HFL1 lung fibrillogenic cells are selected as targets. Based on the differential expression of HA-bound CD44 receptors, the HA-Pt NCs-NH$_2$ could differentially enter into these three kinds of cells and achieving their selective fluorescence imaging of distinguishing types of lung cells. More importantly, Pt NCs significantly inhibited the proliferation, migration and invasion of NSCLC cells and induced their apoptosis in comparison of classical cisplatin and carboplatin, showing a bright future in early diagnosis and treatment of NSCLC.

## 2. Results and Discussion

### 2.1. Synthesis and Characterization of Targeting HA-Pt NCs-NH$_2$

Targeting HA-Pt NCs-NH$_2$ were obtained by the most common EDC/NHS method to combine HA and Pt NCs-NH$_2$ (Scheme 1), and the successful combination of HA and Pt NCs-NH$_2$ was demonstrated by FT-IR measurement (Figure S1). The spectra of HA show the presence of O—H stretching vibrations at 3340 cm$^{-1}$ and C=O stretching vibrations in the carboxyl group at 1604 cm$^{-1}$. The peak of N—H bending vibration for Pt NCs-NH$_2$ is at 1632 cm$^{-1}$, which shifts to 1604 cm$^{-1}$ after HA modification. As for HA-Pt NCs-NH$_2$, the stretching vibration of (O=C—N—H) appears at 1034 cm$^{-1}$ which is not shown in PEI. Moreover, HA-Pt NCs-NH$_2$ are rich in hydrophilic groups such as hydroxyl and amide groups, insuring their good water solubility and dispersibility. The spectra of HA and HA-Pt NCs-NH$_2$ show no significant difference in the positions of most corresponding characteristic absorption peaks, indicating that HA-Pt NCs-NH$_2$ still has the properties of HA after the condensation reaction with PEI. Furthermore, the fluorescent properties of HA-Pt NCs-NH$_2$ were checked and there is no obvious change of fluorescence in comparison with Pt NCs-NH$_2$ (Figure S2).

### 2.2. CD44 Receptor Expression

The expression of HA receptor CD44 on the cell membrane surface was measured using NSCLC 1299 cells, SCLC 446 cells
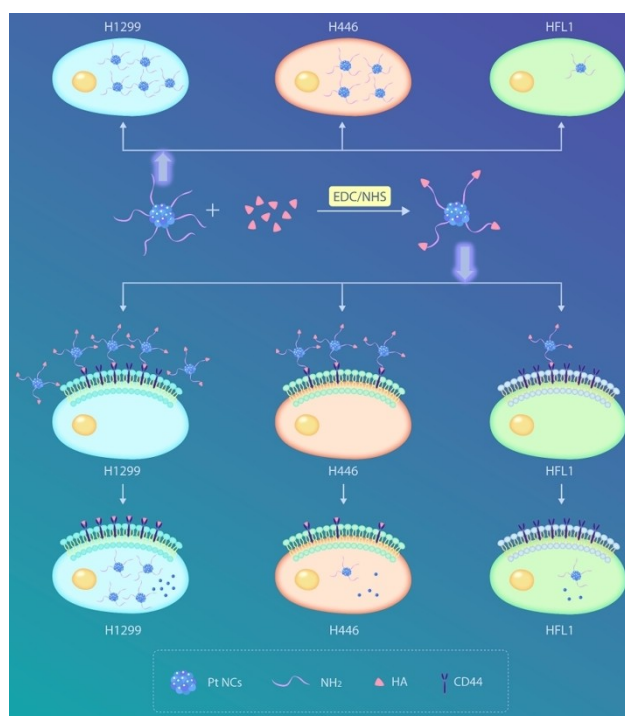


**Scheme 1.** Schematic synthesis of HA-Pt NCs-NH$_2$ and their distinct targeting NSCLC cells H1299, SCLC cells H446 and normal HFL1 lung fibrillogenic cells.

**ChemistryOpen**

Full Papers
doi.org/10.1002/open.202100070

**Chemistry Europe**
European Chemical
Societies Publishing

and normal embryonic lung fibroblasts HFL1 as target cells. To investigate the targeting effect of HA-Pt NCs-NH$_2$ on NSCLC, we assayed the CD44 content on the surface of NSCLC H1299, SCLC H446 cells. As shown in Figure 1, the relative expression of CD44 in H1299 cells was 99.9%, which was significantly higher than the relative expression of 48.8% in H446 cells ($p < 0.001$). It is revealed that HA-Pt NCs-NH$_2$ have the specific trend to express on the membrane surface of NSCLC cells. Normal embryonic lung fibroblasts HFL1 whose relative expression of CD44 on the surface was 98.3%, was employed in order to test the selectivity of unmodified Pt NCs-NH$_2$ and targeting HA-Pt NCs-NH$_2$ between lung cancer cells and normal cells.

## 2.3. Distinct Targeted Labelling of Diverse Cells

Owing to the different expression of CD44, the distinct targeting behaviors of HA-Pt NCs-NH$_2$ on the NSCLC cells H1299, SCLC cells H446 and normal embryonic lung fibroblasts HFL1 were examined (Scheme 1). Figure 2 shows confocal microscopic images of three kinds of cells labelled with Pt NCs-NH$_2$ (before HA modification) and HA-Pt NCs-NH$_2$ (after HA modification), respectively. The green fluorescent signal originated from Pt NCs-NH$_2$ themselves reported in our previous research,[17] while the nuclei are stained with DAPI showing blue fluorescence. After co-culture of Pt NCs-NH$_2$ with these cells for 4 h, it can be seen that there is little difference in the fluorescent intensity of H1299 and H446, and that the proportion of Pt NCs-NH$_2$ entering the cells is comparable and significantly greater than that of normal HFL1 (Figure 2a). Definitely, Pt NCs-NH$_2$ have a favorable ability to selectively bio-imaging the lung cancer and normal cells. As for the HA functioned Pt NCs (HA-Pt NCs-NH$_2$) group, the green fluorescence of H1299 was significantly stronger than that of H446 after HA-Pt NCs-NH$_2$ was co-cultured with cells for 4 h (Figure 2b). It can be seen that HA-Pt NCs-NH$_2$ was able to target NSCLC H1299 cells with high CD44 expression, which is consistent with the results of CD44 detection by flow-through. Meanwhile, the green fluorescence of HFL1 was significantly weaker than that of H1299 and H446 for both Pt NCs-NH$_2$ and HA-Pt NCs-NH$_2$, indicating that our Pt NCs themselves were able to selectively identify cancer cells and only a small amount entered normal lung tissue cells. In sum, Pt NCs-NH$_2$ before and after HA functionality could exhibit the excellent and differ-
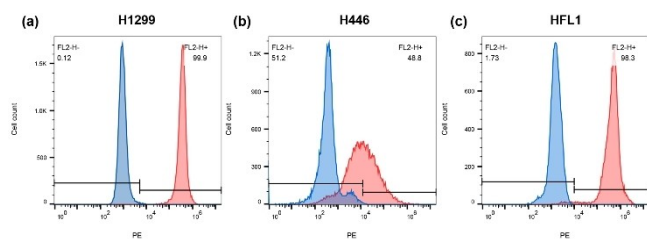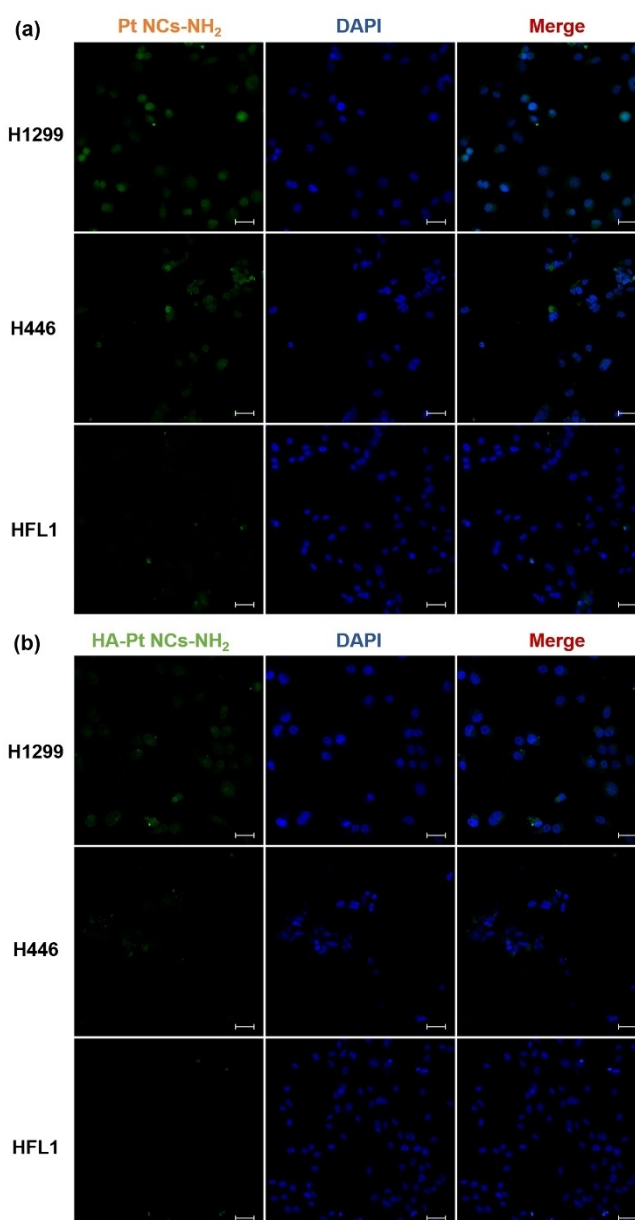


**Figure 2.** Confocal microscopic images of the H1299, H446 and HFL1 cells incubated with (a) Pt NCs-NH$_2$ and (b) targeting HA-Pt NCs-NH$_2$ after 4 h, respectively. Cell nuclei were stained with DAPI which emitted blue fluorescence and Pt NCs-NH$_2$/HA-Pt NCs-NH$_2$ showed green fluorescence. The scale bar is 50 μm.

entiated selectivity and targeting properties against diverse types of cells.

## 2.4. Proliferation Inhibition of NSCLC Cells

In order to investigate the inhibitory effect of targeting HA-Pt NCs-NH$_2$ on NSCLC, the cell proliferation inhibition rate and median inhibitory concentration (IC$_{50}$) were examined by using CCK-8 test. The experiment was set up as the experimental group (Pt NCs-NH$_2$, HA-Pt NCs-NH$_2$, cisplatin and carboplatin),



**Figure 1.** Flow cytometric analysis of CD44 expression in (a) H1299, (b) H446 and (c) HFL1 cells.

control group and blank group. As shown in Figure 3a, the inhibition rates of Pt NCs-NH$_2$ were 39.48%, 79.49%, 83.77% and 83.17% for H1299 cells, and 26.69%, 77.62%, 90.88% and 86.98% for H446 cells when the concentrations ranged from 0.5 to 5.0 μg/mL. There was almost no difference between these two kinds of cancer cells. At the same concentrations, targeting HA-Pt NCs-NH$_2$ inhibited H1299 cells by 26.82%, 65.49%, 79.54% and 88.6%, as well as H446 cells by 4.41%, 14.44%, 33.14% and 67.23%, respectively (Figure 3b). It is greatly obvious that the inhibition rate of H1299 is significantly higher than that of H446. Besides, The IC$_{50}$ of Pt NCs-NH$_2$ was 0.64 μg/mL for H1299 and 0.87 μg/mL for H446, while the IC$_{50}$ of HA-Pt NCs-NH$_2$ was 1.04 μg/mL for H1299 and 3.72 μg/mL for H446. These results further validate the ability of HA-Pt NCs-NH$_2$ to specifically identify NSCLC H1299 cells on account of HA-CD44 interaction. As for normal HFL1 cells, the inhibition rates of Pt NCs-NH$_2$ were 17.94%, 32.34%, 52.72%, and 75.17%, and that of HA-Pt NCs-NH$_2$ were 1.33%, 5.38%, 28.84% and 76.44%, respectively. The IC$_{50}$ of Pt NCs-NH$_2$ and HA-Pt NCs-NH$_2$ against HFL1 cells was 2.32 μg/mL and 3.92 μg/mL. Compared with H1299 and H446, the inhibition rates of both Pt NCs-NH$_2$ and HA-Pt NCs-NH$_2$ were consistently lower for HFL1 in normal cells and did not present the obvious disparity.

Considering the clinical application, the widely used chemotherapeutic drugs, namely cisplatin and carboplatin, were selected to evaluate the inhibitory proliferation of Pt NCs-NH$_2$ and targeting HA-Pt NCs-NH$_2$. As shown in Figure 3c and 3d, the highest inhibition rates of cisplatin and carboplatin on H1299 cells were 12.18% and 4.29% when the concentration was at 5.0 μg/mL. By contrast, the data of inhibition rates for both Pt NCs-NH$_2$ and targeting HA-Pt NCs-NH$_2$ were eight times higher than that of cisplatin and carboplatin at the same concentration. Referring to H446 cells group, the highest

inhibition rates for carboplatin, cisplatin, Pt NCs-NH$_2$ and targeting HA-Pt NCs-NH$_2$ increased gradually from 10.27% to 90.88%. These results demonstrated both Pt NCs-NH$_2$ and targeting HA-Pt NCs-NH$_2$ has a significant superiority in the inhibition of tumor proliferation than classical cisplatin and carboplatin, which showed bright clinical application prospects in future.

## 2.5. Migration and Invasion Inhibition of NSCLC Cells

In general, most tumor cells have a strong ability to migrate, which is an important indicator of metastasis in vivo. In order to investigate whether the targeted HA-Pt NCs-NH$_2$ have an effect on the migration of NSCLC H1299 cell, we inoculated HA-Pt NCs-NH$_2$-treated NSCLC cells on Transwell filter membranes coated with solid matrix chemotactic fibronectin. As shown in Figure 4a, HA-Pt NCs-NH$_2$ treatment significantly reduced the migration of H1299 compared with the control group. Besides, the ability of H1299 migration was obviously reduced with the increase of drug concentration, and the difference was statistically significant. A similar capacity to migration is invasion, and cells with the ability to lyse the cell matrix are usually more invasive. The metastasis of cancer cell requires infiltration and degradation of the extracellular matrix and surrounding tissues around the basement membrane. To exam the role of HA-Pt NCs-NH$_2$ in lung cancer cell invasion, we used a Transwell filter coated with Matrigel, which was used to mimic the basement membrane. From Figure 4b and 4c, it can be seen that HA-Pt NCs-NH$_2$ present a statistically significant decrease in H1299 invasion with increasing the drug concentration from 0.5 to 2.5 μg/mL.
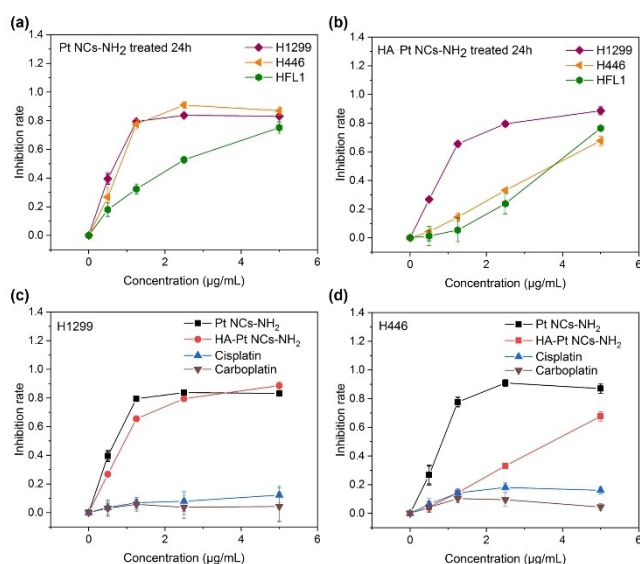


**Figure 3.** Inhibition rate of H1299, H446, and HFL1 cells treated by (a) Pt NCs-NH$_2$ and (b) targeting HA-Pt NCs-NH$_2$ after 24 h; Inhibition rate of (c) NSCLC H1299 cells and (d) SCLC H446 cells after treated by Pt NCs-NH$_2$, targeting HA-Pt NCs-NH$_2$, cisplatin and carboplatin, respectively.
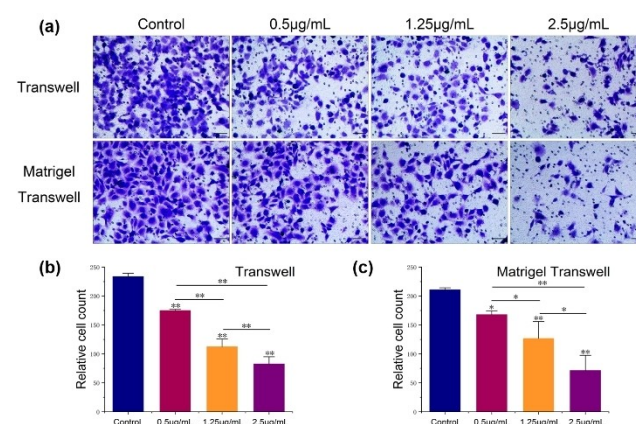


**Figure 4.** (a) H1299 cell migration and invasion assay, experimental group treated with different concentrations of drugs, control group without drugs. The scale bar is 100 μm; (b) Histogram of migration data, the higher the drug concentration, the more pronounced the inhibition of migration; (c) Histogram of invasion assay data, the higher the drug concentration, the more pronounced the inhibitory effect on invasion. *, **, and *** indicate $p < 0.05$, $p < 0.01$, and $p < 0.001$, respectively.

**ChemistryOpen**

Full Papers
doi.org/10.1002/open.202100070

**Chemistry Europe**
European Chemical
Societies Publishing

## 2.6. Induced Apoptosis Mechanism of HA-Pt NCs-NH$_2$ for NSCLC Cells

The apoptosis assay was employed to indicate the apoptotic behaviors of HA-Pt NCs-NH$_2$ on NSCLC cells. As the drug concentration (0.5, 1.25, and 2.5 µg/mL) raised, the relative apoptotic rates of H1299 cells were 40.94%, 84.04% and 92.41% respectively (Figure S3). As can be seen from Figure 5, the relative apoptosis rate of H1299 cells increased dramatically and the relative survival rate decreased significantly when the drug concentration went up from 0.5 to 2.5 µg/mL. The relative apoptotic rate was positively correlated with the concentration of HA-Pt NCs-NH$_2$, and the difference was statistically significant compared with the blank control group ($p < 0.001$). When the concentration of HA-Pt NCs-NH$_2$ was 2.5 µg/mL, the relative apoptosis rate could reach 92.41%, further supporting the results of the previous proliferation inhibition assay.

The proto-oncogene c-myc encodes the transcription factor c-myc, which is important for the control of cell growth and viability. The amount of c-myc is carefully controlled by many mechanisms, and its induction and repression of genes is regulated through interactions with other regulatory proteins. Reduced expression of c-myc and its inappropriate expression may be associated with apoptosis.[19] The expressions of apoptosis-related proteins c-myc were assessed by western blot analysis to investigate the possible mechanism of apoptotic effect on the NSCLC cells. As illustrated in Figure S4, treatment with HA-Pt NCs-NH$_2$ resulted in the downregulation of c-myc ($p < 0.001$), which may be partially responsible for the cell cycle

arrest and apoptotic tendency of the H1299 cells. Recent studies[18] have shown that Pt NCs, a novel Pt-based chemotherapeutic agent, have the superior inhibitory effects on tumor cell proliferation and induction of apoptosis, possibly *via* the activation of p53 protein and related signaling pathways. The mechanism of apoptosis is due to the rapid breakdown of Pt nitrogen compounds into corrosive Pt ions, which tends to bind with DNA and proteins, leading to the destruction of DNA. The present experimental study more comprehensively suggests that HA-Pt NCs-NH$_2$ may induce apoptosis and inhibit proliferation of lung cancer cells by down-regulating the expression of c-myc-related proteins. These results provide an in-depth and reasonable theoretical mechanism for the novel Pt NCs-based chemotherapeutic drugs in the tumor therapy, especially for the NSCLC.

## 3. Conclusion

In summary, we successfully proposed a facile method to synthesized HA functionated Pt NCs-NH$_2$ to form targeting HA-Pt NCs-NH$_2$ chemotherapeutics. Based on the results of confocal microscopic images, HA-Pt NCs-NH$_2$ demonstrated a significate capacity to achieve the selective targeting of NSCLC H1299 cells with the high CD44 expression in comparison of SCLC H446 cells with relative lower CD44 expression due to the specific HA-CD44 interaction. These targeting HA-Pt NCs-NH$_2$ drugs can not only inhibit the proliferation, invasive, and migration ability of H1299 cells, but also dramatically induced apoptosis of NSCLC cells. Moreover, both Pt NCs-NH$_2$ and targeting HA-Pt NCs-NH$_2$ have higher inhibitor rate of both H1299 and H446 cells in comparison with commonly-used chemotherapy drugs (e.g. cisplatin and carboplatin). The apoptosis mechanism possibly is that HA-Pt NCs-NH$_2$ induced the down-regulating expression of c-myc-related proteins in NSCLC system. Depend on the merits of HA-Pt NCs-NH$_2$ such as accurate targeting, unique selectivity and better efficacy, it can be predicted that this kind of Pt NCs-based chemotherapeutics will exhibit a promising potential in the diagnosis and treatment of NSCLC.

## Experimental Section

### Materials

NSCLC H1299 cells, SCLC H446 cells, and human embryonic lung fibroblasts HFL1 were purchased from the Institute of Cell Research, Chinese Academy of Sciences (Shanghai, China). 4′,6-diayl-2-phenyl-indole (DAPI) was brought from Solarbio (Beijing, China). CD44 antibody was procured from Elabscience (Wuhan, China). Cisplatin and carboplatin were obtained from Qilu Pharmaceutical (Jinan, China). C-myc antibody was supplied by Sanying (Wuhan, China). Beta Aactin (AF7018) and goat anti-Rabbit IgG (H + L) HRP (S001) were purchased from Affinity Biosciences. Sodium Hyaluronate (HA), 1-(3-dimethylaminopropyl)-3-ethylcarbodiimide hydrochloride (EDC) and N-hydroxysuccinimide (NHS) were acquired from China Pharmaceutical Group (China).
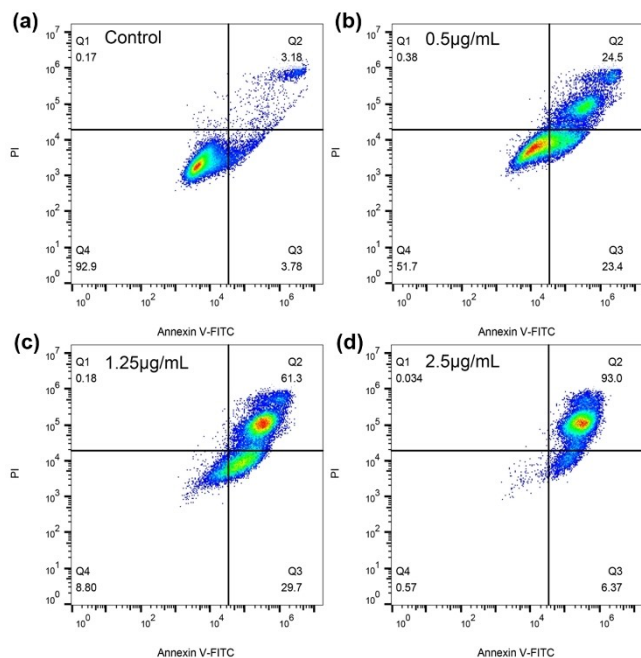


**Figure 5.** HA-Pt NCs-NH$_2$ induced apoptosis in H1299 cells. Q1-Q4 are necrotic cells, late apoptotic cells, early apoptotic cells and live cells, respectively. (a) stands for the control group and (b–d) are experimental groups treated with different drug concentrations from 0.5 to 2.5 µg/mL. The relative apoptosis formula is as follows: relative apoptosis rate = actual apoptosis rate – control apoptosis rate.

**ChemistryOpen**

**Full Papers**
doi.org/10.1002/open.202100070

**Chemistry Europe**
European Chemical
Societies Publishing

## Construction and Characterization of Targeting HA-Pt NCs-NH$_2$

Fluorescent Pt NCs-NH$_2$ with the emission wavelength at 558 nm under the excitation wavelength at 460 nm, were synthesized by the reported one-pot method.[17] HA-Pt NCs-NH$_2$ was prepared as follows: HA was dissolved in 10 mL of distilled water with sufficient stirring at 37 °C, cooled to room temperature and EDC was added for 10 min shaking and NHS was added for another 60 min shaking at 37 °C, respectively. Then Pt NCs-NH$_2$ solution was added and shaken overnight at 37 °C. The pre-product was treated by centrifugation. A dialysis bag ($M.W. = 1000$ D) was selected to remove unreacted EDC, NHS and HA overnight, and the supernatant was centrifuged by the ultrafiltration tube ($M.W. = 3000$ D) twice for 15 min. The samples were collected and stored at 4 °C under protection against the light. Fourier infrared spectroscopy (FT-IR, Thermo Scientific Nicolet iS10, USA) measurements in ATR mode were selected to detect whether the HA was successfully modified, while the fluorescent properties were tested by F7000 spectrofluorometer (Hitachi Limited, Japan).

## Cell Culture

NSCLC cells H1299, SCLC cells H446 and normal HFL1 lung fibrillogenic cells were cultured in Dulbecco's Modified Eagle Medium (DMEM, GIBCO, New York, USA) containing 10 % fetal bovine serum (FBS, GIBCO, New York, USA). All cells were incubated in a humidified atmosphere at 37 °C and 5 % CO$_2$ and passaged once every 2–3 days.

## Detection of CD44 Receptor Expression by Flow Cytometry

H1299, H446 and HFL1 cells were collected by digestion, washed at least once with phosphate buffer wash PBS (Sigma Aldrich, St. Louis, MO, USA) stained by adding 5 μL phycoerythrin (PE) anti-human CD44 antibody. Staining was usually performed at room temperature and protected from light for 15–30 min, and the volume of chromosome lines was usually in the range of 100–500 μL, washed at least twice after completion of staining, centrifuged for 5 min. The supernatant was discarded, and the sample was diluted to 500–1000 μL by adding PBS for examination.

## Detection of Uptake of Pt NCs-NH$_2$ and HA-Pt NCs-NH$_2$

The experiment was divided into three groups, namely H1299 group, H446 group and HFL1 group. All cells were incubated in glass petri dishes (NEST, 35 mm, China) at a density of $1 \times 10^5$/mL and cultured for 24 h before various treatments were performed. Pt NCs-NH$_2$ (5 μg/mL) and HA-Pt NCs-NH$_2$ (5 μg/mL) were added to each group of cells and incubated for 4 h. Cells were fixed with 4 % paraformaldehyde, washed with PBS, and then the nuclei were stained with DAPI (10 μg/mL) for 10 min at room temperature and then washed again with PBS three times. The samples were observed by confocal microscope (lsm830, Zeiss, GER) at 488/560 nm (excitation/emission), and the observation multiple was $20 \times 10$.

## Cell Counting Kit 8 (CCK-8) Test

The CCK-8 test consists of four groups for each cell, H1299 + Pt NCs-NH$_2$, H1299 + HA-Pt NCs-NH$_2$, H1299 + cisplatin and H1299 + carboplatin. The H446 and HFL1 are grouped as same as H1299. Each group of cells was cultured in 96-well plate dishes at a density of $1 \times 10^4$/mL for 24 h. Then, Pt NCs-NH$_2$, HA-Pt NCs-NH$_2$, cisplatin and carboplatin were added at different concentrations for another

24 h. Finally, CCK-8 (Abmole Bioscience, USA) was added for the co-incubation. The mean optical density and inhibition were counted at 450 nm by universal microplate spectrophotometer (ENSIGHT, PerkinElmer, Waltham, MA, USA).

## Apoptosis Assay

The Annexin V-FITC apoptosis kit (BD Pharmingen, USA) and flow cytometer (BD Accuri C6: BD Biosciences, San Jose, CA, USA) were used to detect the cell apoptosis. Experimental and control groups were set up. Cells from each group were grown at a density of $1 \times 10^5$/mL in 6-well plate dishes for 24 h. Subsequently, the cells were co-incubated with different concentrations of HA-Pt NCs-NH$_2$ at 0.5, 1.25 and 2.5 μg/mL. Cells were collected and washed with PBS, transferred to test tubes and stained with a membrane linked protein V/PI staining protocol. All samples were analyzed by flow cytometry. Fluorescence emission was measured at 530 nm and 575 nm when it was excited at 488 nm. Data were processed using Flow JO 10.6.

## Transwell Migration and Invasion Assay

The upper chamber surface of the bottom membrane of the Transwell was coated with 50 mg/L Matrigel dilution (Matrigel: DMEM = 1:8) and placed at 37 °C for 30 min before use (this step was ignored for migration assays). H1299 cells were counted after 24 h of serum-free starvation culture, resuspended in serum-free medium, and the cell concentration was adjusted to $1 \times 10^5$/mL. The cells were treated with different concentrations of HA-Pt NCs-NH$_2$ at 0.5, 1.25 and 2.5 μg/mL, and left for 12 h. The cells were washed twice with PBS solution and then wiped off. The upper layer of cells was fixed with formaldehyde for 20 min, then stained with staining solution containing 0.1 % crystal violet for 15–20 min and rinsed three times with PBS. The average number of cells was calculated by randomly taking 6–8 fields of view under an inverted microscope.

## Western Bolt

H1299 cells were incubated for 24 h in culture dishes (6-well plates) spiked with HA-Pt NCs-NH$_2$ (0 and 2.5 μg/mL) at a density of $1 \times 10^5$/mL. Cellular protein collection and protein quantification were then performed for later experiments. Subsequent steps were as follows: SDS gel preparation, sample loading, electrophoresis, membrane transfer, antibody incubation, chemiluminescence and fixation.

## Statistical Analysis

Statistics were performed using SPSS19. 0 software (SPSS, US), and the measured data were expressed as mean ± standard deviation, and the differences between groups were compared by one-way ANOVA. Independent samples t-test was used for comparison between the two groups, and $p < 0.05$ was considered as a statistically significant difference.

**ChemistryOpen**

Full Papers
doi.org/10.1002/open.202100070

**Chemistry Europe**
European Chemical
Societies Publishing

## Conflict of Interest

The authors declare no conflict of interest.

[1] a) D. Youlden, S. Cramb, P. Baade, *J. Thorac. Oncol.* **2008**, *3*, 819–831; b) F. Bray, J. Ferlay, I. Soerjomataram, R. Siegel, L. Torre, A. Jemal, *Ca-Cancer J. Clin.* **2018**, *68*, 394–424.

[2] a) R. Pirker, *Curr. Opin. Oncol.* **2020**, *32*, 63–67; b) S. Sörenson, B. Glimelius, P. Nygren, *Acta Oncol.* **2001**, *40*, 327–339.

[3] a) O. Abdifetah, K. Na-Bangchang, *Int. J. Nanomed.* **2019**, *14*, 5659–5677; b) M. Maurel, T. Montheil, J. Martin, L. Chaar, V. Guzman-Gonzalez, M. Couvet, T. Jacquet, T. Jia, B. Eymin, K. Parra, P. Dumy, J. Martinez, F. Ruggiero, E. Vaganay, A. Mehdi, J. Coll, G. Subra, *Nanomaterials (Basel)* **2021**, *11*; c) B. Le Droumaguet, J. Nicolas, D. Brambilla, S. Mura, A. Maksimenko, L. De Kimpe, E. Salvati, C. Zona, C. Airoldi, M. Canovi, M. Gobbi, N. Magali, B. La Ferla, F. Nicotra, W. Scheper, O. Flores, M. Masserini, K. Andrieux, P. Couvreur, *ACS Nano* **2012**, *6*, 5866–5879.

[4] a) P. Kumari, B. Ghosh, S. Biswas, *J. Drug Targeting* **2016**, *24*, 179–191; b) E. Pérez-Herrero, A. Fernández-Medarde, *Eur. J. Pharm. Biopharm.* **2015**, *93*, 52–79.

[5] a) M. Alavi, M. Hamidi, *Drug Metab. Pers. Ther.* **2019**, *34*; b) B. Bayram, A. Ozgur, L. Tutar, Y. Tutar, *Curr. Pharm. Des.* **2017**, *23*, 5349–5357; c) N. Muhamad, T. Plengsuriyakarn, K. Na-Bangchang, *Int. J. Biol. Macromol.* **2018**, *13*, 3921–3935.

[6] K. W. Yong, D. Yuen, M. Z. Chen, A. P. R. Johnston, *ACS Appl. Mater. Interfaces* **2020**, *12*, 5593–5600.

[7] M. Srinivasarao, P. Low, *Chem. Rev.* **2017**, *117*, 12133–12164.

[8] a) M. Hemshekhar, R. M. Thushara, S. Chandranayaka, L. S. Sherman, K. Kemparaju, K. S. Girish, *Int. J. Biol. Macromol.* **2016**, *86*, 917–928.

[9] H. Ponta, D. Wainwright, P. Herrlich, *Int. J. Biochem. Cell Biol.* **1998**, *30*, 299–305.

[10] a) I. Caon, B. Bartolini, A. Parnigoni, E. Caravà, P. Moretto, M. Viola, E. Karousou, D. Vigetti, A. Passi, *Semin. Cancer Biol.* **2020**, *62*, 9–19; b) L. Prochazka, R. Tesarik, J. Turanek, *Cell. Signalling* **2014**, *26*, 2234–2239; c) G. Mattheolabakis, L. Milane, A. Singh, M. Amiji, *J. Drug Targeting* **2015**, *23*, 605–618.

[11] a) C. da Cunha, C. Oliveira, X. Wen, B. Gomes, S. Sousa, G. Suriano, M. Grellier, D. Huntsman, F. Carneiro, P. Granja, R. Seruca, *Lab. Invest.* **2010**, *90*, 1604–1614; b) V. Orian-Rousseau, H. Ponta, *Arch. Toxicol.* **2015**, *89*, 3–14; c) S. Ghosh, S. Neslihan Alpay, J. Klostergaard, *Expert Opin. Ther. Targets* **2012**, *16*, 635–650.

[12] C. Chen, S. Zhao, A. Karnad, J. Freeman, *J. Hematol. Oncol.* **2018**, *11*, 64.

[13] Y. Ren, T. Zhao, G. Mao, M. Zhang, F. Li, Y. Zou, L. Yang, X. Wu, *Int. J. Biol. Macromol.* **2013**, *57*, 57–62.

[14] a) M. El-Dakdouki, J. Xia, D. Zhu, H. Kavunja, J. Grieshaber, S. O'Reilly, J. McCormick, X. Huang, *ACS Appl. Mater. Interfaces* **2014**, *6*, 697–705; b) W. Li, X. Yi, X. Liu, Z. Zhang, Y. Fu, T. Gong, *J. Controlled Release* **2016**, *225*, 170–182; c) L. Zhong, X. Xu, Y. Liu, Q. Li, D. Zhao, Z. Li, H. Zhang, H. Zhang, Q. Kan, Y. Wang, J. Sun, Z. He, *Acta Pharm. Sin. B* **2019**, *9*, 397–409.

[15] H. Yoon, H. Koo, K. Choi, S. Lee, K. Kim, I. Kwon, J. Leary, K. Park, S. Yuk, J. Park, K. Choi, *Biomaterials* **2012**, *33*, 3980–3989.

[16] a) L. Zou, X. Song, T. Yi, S. Li, H. Deng, X. Chen, Z. Li, Y. Bai, Q. Zhong, Y. Wei, X. Zhao, *Cancer Gene Ther.* **2013**, *20*, 242–250; b) W. Huang, J. Lin, J. Hsieh, S. Chou, C. Lai, E. Yun, U. Lo, R. Pong, J. Lin, Y. Lin, *ACS Appl. Mater. Interfaces* **2016**, *8*, 30722–30734.

[17] X. Chen, J. Zhou, X. Yue, S. Wang, B. Yu, Y. Luo, X. Huang, *Biochem. Biophys. Res. Commun.* **2018**, *503*, 1465–1470.

[18] Y. Xin, X. Huang, Z. Li, W. Zhao, C. Wang, S. Wang, X. Yue, H. Mo, H. Li, *Biochem. Biophys. Res. Commun.* **2019**, *512*, 218–223.

[19] Thompson, E. Brad, *Annu. Rev. Physiol.* **1998**, *60*, 575–600.

[20] D. Pedone, M. Moglianetti, E. De Luca, G. Bardi, P. Pompa, *Chem. Soc. Rev.* **2017**, *46*, 4951–4975.